

L. W. Li¹, T. L. Dong¹, W. T. Ji², J. M. Wu^{1*}

State Key Laboratory for Strength and Vibration of Mechanical Structures Shaanxi Key Laboratory of Environment and Control for Flight Vehicle School of Aerospace, Xi'an Jiaotong University Xi'an, Shaanxi, China
Key Laboratory of Thermo-Fluid Science and Engineering of MOE School of Energy and Power Engineering, Xi'an Jiaotong University Xi'an, Shaanxi, China

Abstract

Pin-fins are widely used to cool the trailing edge of the rotor and stator blades, which could enhance the heat transfer by increasing the heat transfer area and the turbulence intensity of cooling air. In current study, relatively large aspect ratio pin-fin arrays (the height-to-diameter ratio of the pins is 2.5) are investigated numerically through a range of Reynolds numbers between 5,000 and 50,000 to determine the effects of shape and streamwise spacing on the heat transfer augment ability and array friction factor in the channel. Staggered pin-fins of different cross-sectional shapes (circular, elliptic and teardrop) are studied in a rectangular channel with the aspect ratio of 4.8:1, and the ratio of streamwise spacing to diameter (X/d) varies from 2.0 to 3.0. Current results show that the overall performance of the elliptical-shaped pin-fin is better than the other two pin-fins, and the pins with X/d = 2.0 behave relatively better in flow and heat transfer performance when considering the variation of X/d of the elliptic pin-fin. Moreover, for the elliptical pin-fins with H/d = 2.5 in this study, Nu_p is less affected by streamwise spacing than Nu_e , and the ratio of $Nu_{p,ave}/Nu_{e,ave}$ ranges from 1.30 to 1.65 for the elliptic pin-fins studied in this article.

Keywords: gas turbine; trailing edge cooling; pin-fins; heat transfer characteristic; flow resistance

1. Introduction

Gas-turbine engines can achieve greater thermal efficiency by increasing the turbine inlet temperature according to the Brayton cycle. The increase rate of turbine inlet temperature is much faster than the development rate of blade materials with higher heat resistance performance, which presents as a challenge for the operating of turbine vane and blade. Especially, trailing-edge cooling for gas turbine blade is of high degree of attention for designers due to its critical operation conditions. Previous studies show that the thin trailing edge weakens the structural strength of the blade. Moreover, the complex flow structures such as shock/expansion waves and unsteady wakes result in high heat load in the trailing edge region [1]. The pin-fin arrays are generally used at the trailing edge of the blade to improve the mechanical strength as well as the cooling performance by increasing the heat transfer area and the turbulence intensity of cooling air.

As a simplified model of internal cooling passage of gas turbine blade at the trailing edge, previous studies have revealed the typical flow and heat transfer characteristics for pin-fin arrays in the rectangular channel, which involved the effect of the pin-fin arrangement, the pin-fin spacing, and the pin-fin shape. Chyu et al. [2] reported that the heat transfer coefficient of the staggered arrays is higher than that of the in-line arrangement. Lawson et al. [3] presents that both the decrease of the spanwise and the streamwise spacing enhance the heat transfer. Streamwise spacing has greater influence on the heat transfer of the channel, while spanwise spacing shows greater impact on the flow resistance of the channel. Ostanek et al. [4] measured the time-dependent near wake flow and found that the vortex shedding observed for spanwise spacings larger than 2 is beneficial for heat

transfer on the pin surface.

Researchers have also carried out some outstanding work on the effect of pin-fin shape. At present, the shape of pin-fins is roughly divided into the ones with continuous cross-sectional curvature, such as circular, elliptical and teardrop, and the ones with discontinuous curvature, such as triangle and diamond. Studies have found that despite the former have a weaker heat transfer ability, the pressure drop is lower than the latter ones. Chen et al. [5] revealed that the channel with drop-shaped pin-fins shows higher heat transfer rate and a smaller pressure loss than the channel with cylindrical pin-fins. Sahiti et al. [6] numerically investigated six forms of pin cross-section under relatively low Reynolds number ranging from 100 to 1000, which shows that the staggered arrangement of the elliptic profile performs better than all other pin cross-sections. Uzol et al. [7] observed a larger region of a low speed wake behind the circular pin-fins, which leads to 46.5% higher than elliptical pin-fins in pressure loss. Xu et al. [8] compared the performance of nine sets of pin-fins and discovered that the Diamond-s pin-fins presents the best overall thermal performance on the endwall for all the nine pin-fins under different Reynolds numbers, and the characteristic of local heat transfer distribution varies substantially for different pin-shapes at low Reynolds number, which has similar results with Corbett's study.[9].

Height-to-diameter ratio of the pin-fin is regarded as a crucial factor affecting the heat transfer performance by the surface area participating in heat transfer. Pin-fins commonly used in actual turbine blade cooling have pin height-to-diameter ratio between 0.5 and 4. VanFossen et al. [10] found that the row-averaged heat transfer coefficient is more sensitive to the variation of height-to-diameter ratio for short pin-fins (H/d < 2.0) than longer pin-fins. Chyu et al. [11] tested pin-fins with H/d ratios ranging from 2.0 to 4.0 when Reynolds number varies from 10000 to 30000 and concluded that the increase of the pin height leads to the enhancement of the overall array-averaged heat transfer and greater pressure loss. In addition, most of the heat transfer contribution comes from the pins rather than the endwall for pins with H/d > 2. It is noted that in industrial manufacturing, heavy-duty gas turbine blades are normally much larger than blades of aero-engines [12], which gives much more freedom for designing the cooling structures inside the cooling passage. However, many studies have focused on the research with low aspect ratio pin-fins (H/d = 1) [13-18]. As a result, special focus should be given to pin-fins with large aspect ratios to meet the requirements when studying internal cooling in heavy-duty gas turbine blades.

Heat transfer in a turbine pin-fin array combines the cylinder heat transfer and endwall heat transfer. Early investigations on the performance of pin-fin arrays identified the independent impacts that the pins and endwall surfaces had on the total heat transfer. Metzger et al. [16] suggested that the pin surface heat transfer coefficient is about double the endwall value for 2.5 < S/d < 3.5, 1.5 < X/d < 3.5, and H/d = 1. Chyu et al. [17] reported that for H/d = 1 and S/d = X/d = 2.5, the pin surface has about 10% to 20% higher heat transfer coefficient than the endwall. Lyall et al. [18] researched the heat transfer of endwall and pin-fins respectively (Nu_e , Nu_p) in the rectangular channel placing a single row of pin-fin under different spanwise spacings. They found that the Nu_e/Nu_p gradually decreased to a constant value when the Reynolds number increases, and this ratio raises with the increase of the spanwise ratio.

When evaluating the heat transfer of the pin surface, some researchers selected copper as the material of pin-fins, which brings convenient to evaluate the surface temperature due to its high thermal conductivity. However, the thermal conductivity variation leads to different fluid-solid thermal resistance, which directly influences the conjugated heat transfer performance on the pin-surface. If experiments and numeration are adopted to simulate the real pin-fin channel, the pin-fin thermal conductivity coefficient (or materials) used by the researchers should be chosen carefully according to the Biot number consistency principle [19]. Wright et al. [20] investigated the enhancement due to both conducting (copper) pin-fins and nonconducting (Plexiglas) pins in stationary and rotation conditions. It was demonstrated that the Nusselt number ratios for the conducting pin-fin channel are greater than those of the nonconducting pin-fin channels, and the ratios of the two channels increased at the same rate as the rotation number increases. Li et al. [21] explored the effect of thermal conductivity of different pin-fin materials (Perspex, ceramic glass and stainless steel) on the temperature and Nusselt distribution of the endwall, which suggested that lower thermal conductivity results in higher heat pick-up ability in the fluid-solid interface, but It also contributes to higher thermal

gradient along the wall thickness.

Therefore, one of the objectives of this study is to establish numerical models which take the cylinder heat transfer into consideration by utilizing relatively large aspect ratio pin-fin arrays and choosing appropriate pin-fin material. Secondly, the work will examine the effect of the pin-fin shape (circular, elliptic, teardrop) and pin-fin spacing on the flow characteristics and heat transfer performance in the static rectangular channel. At the same inlet Reynolds number and temperature ratio condition, the heat transfer and flow characteristics for the channel with different shapes of pin-fins are compared and analyzed. After choosing the best-performed-shape by comparing the overall thermal performance, the study focus on the effect of streamwise spacing on the flow and heat transfer characteristics. In addition, since the model involves the heat transfer on both endwall and the pin surface, the heat transfer on each region will be investigated individually in this part.

The remainder of this paper is organized as follows. First, the physical models are described. This is followed by the numerical method of solution, a grid sensitivity study, and a validation study. Afterwards, the results are presented.

2. Physical Models

2.1 Model Used in Checking the Effect of Pin-fin Shape

Wright et al. [20] experimentally studied the effect of pin-fins conductivity on the heat transfer characteristics for circular pin-fin arrays by the copper plate regional average method in 2004. The copper plates embedded with thermocouples are heated with thin heaters underneath to provide a locally constant heat flux. As copper is an excellent conductor of heat, the measured wall temperatures are considered as regionally averaged, and the heat-transfer coefficient is then calculated. The study simulates the coolant stream flowing upward from the blade root. The pin-fin distribution in his work is shown in Figure 1(a), which has 12 rows of staggered pin-fins. And the streamwise and spanwise spacing-to-diameter ratios (X/d, S/d) are 2, the height to diameter ratio is also set to 2. Reynolds number varies from 5×10^3 to 2×10^4 .

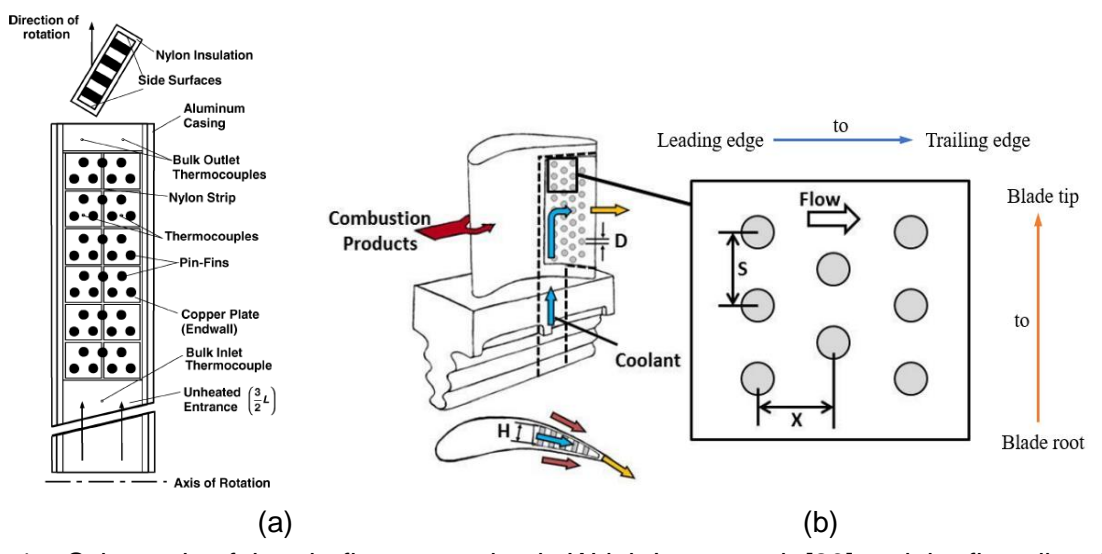


Figure 1 – Schematic of the pin-fin test section in Wright's research [20] and the flow direction in pin-fin channel in real blade.

The basic model in the present work refers to the model of Wright's. In the present study, to study the flow in the direction from the leading edge to the trailing edge, the row number is declined to 6, and the number of pin-fins in each row becomes larger. For the heating of test section, one should note that the copper plate heated with thin heaters underneath in Wright's experiment is simplified as the copper block region with constant heat source in the present work. Moreover, the copper block regions on one side of channel are merged as a single copper region, neglecting the unheated strips between the plates, which is closer to the actual heating condition in typical turbine blades.

The detailed computational model with pin-fins in different shapes is shown in Figure 2. The fluid domain is wrapped by the insulation made by PC (Polycarbonate), and each of the copper plates is mounted into this insulation, as illustrated in Figure 2(a). For the fluid domain, extended channels

are placed downstream of the heated channel to avoid backflow, and upstream of the heated channel to ensure the full development of the fluid at the inlet of the heated channel. Therefore, the fluid domain includes three sections: inlet (L_{in}) , heated (L) and outlet (L_{out}) . In Figure 2, x coordinate indicates the channel length's direction from inlet, y coordinate indicates the channel wideness's direction and z coordinate indicates the channel height's direction from the bottom surface.

The pin-fin distribution in this work is shown in Fig. 2(b), which has 6 rows of staggered pin-fins. And the streamwise spacing-to-diameter ratio (X/d) is 2, the spanwise spacing-to-diameter ratio (X/d) is also 2, the height-to-diameter ratio (X/d) is 2.5. Reynolds number based on hydraulic diameter of the channel (24.83 mm) varies from 5×10^3 to 5×10^4 . Table 1 shows the geometrical sizes of channel and pin-fins.

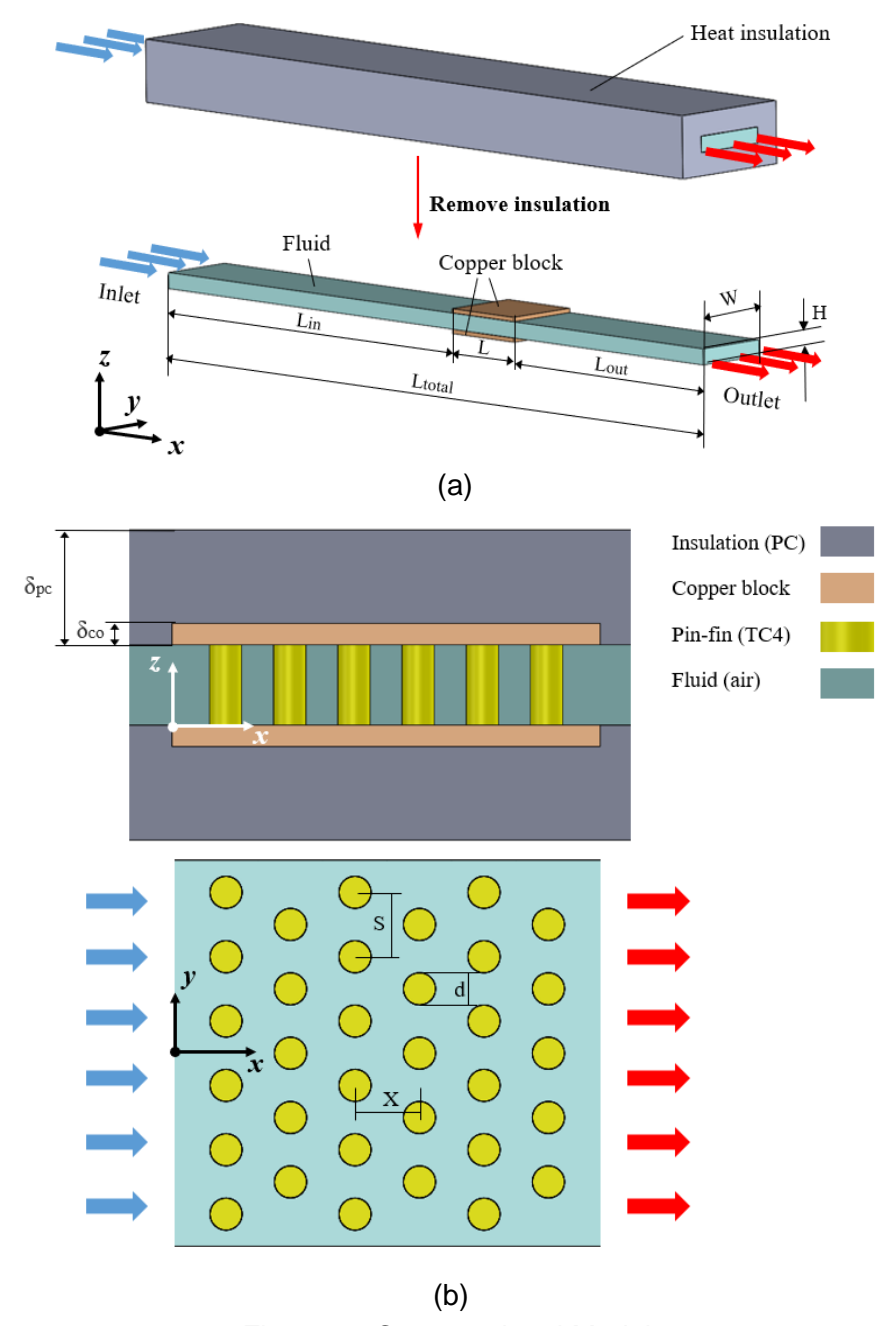


Figure 2 - Computational Model.

Table 1 –Geometrical sizes of channel and pin-fins for Fig. 2 (units: mm).

Parameter	Value	Parameter	Value
L_{total}	691	δ_{pc}	21.5
L_{in}	374	δ_{co}	4

Table 1 (continued) –Geometrical sizes of channel and pin-fins for Fig. 2 (units: mm).

Parameter	Value	Parameter	Value
L	80	d	6
L_{out}	237	X/d	2
H	15	S/d	2
W	72	H/d	2.5

Based on the model with circular pin-fins, the other two models with pin-fins in different shapes (elliptic and teardrop) are designed. It should be noticed that the maximum wideness of the two pin-fins have the same value as the circulars' diameter, and six rows of staggered pin-fins are arranged in the heated channel, as shown in Figs. 2 and 3. The overall streamwise length of elliptic and teardrop are 1.67 times as the diameter of circular.

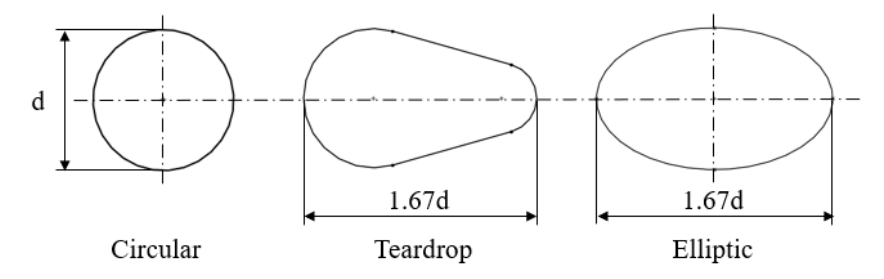


Figure 3 – Shape and sizes of cross section of different kind of pin-fins.

2.2 Model Used in Checking the Effect of Pin-fin Streamwise Spacing

The results from the study on the effect of pin-fin shapes on flow and heat transfer characteristics of the channel reveal that the elliptic pin-fins have better overall thermal performance in present work, as shown in section 5.1.2. Therefore, the present paper selects elliptic pin-fins to study the effect of the pin-fin streamwise spacing on the flow and heat transfer characteristics of the channel. In present study, the pin-fin's wideness, row number and the fluid domain length of L_{total} , wideness of W and height of H remain unchanged. The ratio of streamwise spacing to the diameter (X/d) of elliptic pin-fins is set to be 2, 2.5 and 3. Therefore, it's easy to suppose that the length of the inlet (L_{in}) , heated (L) and outlet (L_{out}) sections of the computational channel have different values, as shown in Table 2.

Table 2 –Geometrical sizes of channel and pin-fins with different streamwise spacing.

		Cha	nnel				F	Pin-fins		
L_{total}	Н	W	L	L_{in}	L_{out}	Shape	d	X/d	S/d	H/d
[mm]	[mm]	[mm]	[mm]	[mm]	[mm]		[mm]			
691	15	72	80	374	237	Elliptic	6	2	2	2.5
			95	364	232			2.5		
			110	354	227			3		

3. Governing Equations and Boundary Conditions

This calculation focuses on the resistance brought by the pin-fins as a turbulence generator to the flow of air in the channel and its enhancement on the cooling for the total heat transfer area. Therefore, in the calculation, the thermal conductivity inside the pin-fin is coupled with the convective heat transfer in the fluid region. The governing equations used are as follows:

Continuity equation in fluid domain:

$$\frac{\partial(\rho u_i)}{\partial x_i} = 0 \tag{1}$$

Momentum equation in fluid domain:

$$\rho u_{j} \frac{\partial u_{i}}{\partial x_{i}} = -\frac{\partial p}{\partial x_{i}} + \frac{\partial}{\partial x_{i}} (\mu \frac{\partial u_{i}}{\partial x_{j}}) + \frac{\partial}{\partial x_{i}} (-\rho \overline{u_{i}^{\prime} u_{j}^{\prime}})$$
(2)

Energy equation in fluid domain:

$$\rho u_j \frac{\partial T}{\partial x_j} = \frac{1}{C_p} \frac{\partial}{\partial x_j} (\lambda \frac{\partial T}{\partial x_j})$$
(3)

Conduction equation in the pin-fin:

$$\frac{\partial^2 T}{\partial x_i x_j} = 0 \tag{4}$$

Conduction equation in the copper block:

$$\lambda \frac{\partial^2 T}{\partial x_i x_i} + S = 0 \tag{5}$$

Table 3 shows the computational domain condition and the boundary conditions for Fig.2. The flow state is steady. The two endwalls are heated by the constant heat source, and the other walls are coupled. For the pin-fin material, titanium alloy (TC4) is selected according to reference [22], in order to ensure the nondimensional temperature distribution of the numerical model aligned with that of the actual model.

Computation	onal Domain Condition	Boundary Condition		
Fluid	Compressible air	Inlet	Mass-flow-inlet from <i>Re</i> uniform temperature of 293 K	
Copper block	Copper, with constant heat source, keeping $T_{w,ave}/T_{in} = 1.1$	Outlet	Pressure-outlet with gauge pressure of 0 Pa	
Pin-fin	TC4, $\lambda = 7.4 \text{ W/(m·K)}$	External walls	Convective, with free stream temperature of 293 K, heat transfer coefficient of 5 W/(m²·K)	
Heat insulation	PC, $\lambda = 0.25 \text{ W/(m·K)}$	Other fluid-to- solid walls	Coupled and non-slip boundary	
-	-	Solid-to-solid	Coupled	

Table 3 –Computational domain and boundary conditions.

4. Numerical Method and Some Details

4.1 Data Processing

Two kinds of definitions of Reynolds number and Nusselt number are used in this study as follows: For the overall thermal performance evaluation:

walls

Channel Reynolds number and channel Nusselt number are typically used to characterize heat transfer and flow when discussing augmentation based on the correlated smooth channel Nusselt number (Nu_0) .

Channel Reynolds number based on inlet condition is defined as

$$Re = \frac{\rho_{in}u_{in}D_h}{\mu_{T_{in}}} \tag{6}$$

Where ρ is the air density, $kg \cdot m^{-3}$. u is channel inlet velocity, $m \cdot s^{-1}$. D_h is channel hydraulic diameter, m. μ is dynamic viscosity, $Pa \cdot s$.

The channel heat transfer coefficient is defined as

$$h_{ave} = \frac{Q_{net} / A}{T_{w,ave} - T_{b,ave}} \tag{7}$$

Where Q_{net} is the total heat entering the flow which combines the heat transfer from the pin surface and the endwalls, W. A is the heated area of the smooth channel with pin-fins uninstalled $(2\times W\times L)$, m^2 . T_w is the temperature of the heated wall, K. And T_b is the bulk air temperature of the heated section, K.

The channel Nusselt number is defined as

$$Nu_{ave} = \frac{h_{ave}D_h}{\lambda} \tag{8}$$

Where λ is the fluid thermal conductivity based on T_b , $W \cdot m^{-1} \cdot K^{-1}$.

For the individual evaluations of the performance of pins and the endwall surfaces:

Reynolds number based on the pin diameter is typically utilized in the present study to calculate Nusselt number on the pins and endwall surfaces, which is defined as

$$Re_d = \frac{\rho U_{max} d}{u} \tag{9}$$

Where d is the diameter or maximum wideness of the pin-fin, m. U_{max} is the mean velocity across the minimum cross-sectional area, $m \cdot s^{-1}$.

Table 4 shows the comparison between the Reynolds numbers based on the hydraulic diameter and the pin diameter.

Table 4 –Comparisons between the Re and the Re_d .

Re	5000	10000	20000	30000	40000	50000
Re_d	2416	4832	9665	14498	19331	24164

The local heat transfer coefficient is defined as

$$h = \frac{q}{T_{\dots} - T_{b_{\dots} J_b}} \tag{10}$$

Where q is the heat flux of the surface, W·m⁻². T_{bulk} is the local fluid bulk temperature, K, which is calculated by a linear interpolation between the inlet and outlet temperature of the test section.

The pin or endwall Nusselt number is defined as

$$Nu_d = \frac{hd}{\lambda} \tag{11}$$

The friction factor of the channel is defined as

$$f = \frac{\Delta p D_h}{0.5 \rho_{in} u_{in}^2 L} \tag{12}$$

Where Δp is pressure drop across the heated channel, Pa.

4.2 Meshing and Grid Independence Analysis

In this paper, the computational domain is set up with hexahedral structure grids, as shown in Fig. 4. Boundary layer grids are drawn around the pin-fins and near all the walls of the channel, Considering the accurate prediction of turbulence flow, the height of first-layer of boundary layer grids is set to be small enough to satisfy the criterion that y+ value be close to 1 for the current study.

The average Nusselt number on the heated wall is computed for the channel with circular pin-fins (Model of Fig. 2) at the condition of Re = 5,000 under four grid systems (4.28, 7.72, 9.40 and 11.35 million) to verify grid independence. The results are shown in Fig. 5. It is found that when the grid number exceed 9.40 million, the average Nusselt number increases very slowly, which indicates that grid number around 9.40 million should be acceptable for obtaining grid-independent solution and saving computing time. Therefore, the generated mesh in the following different cases all include about 9.40 million grids.

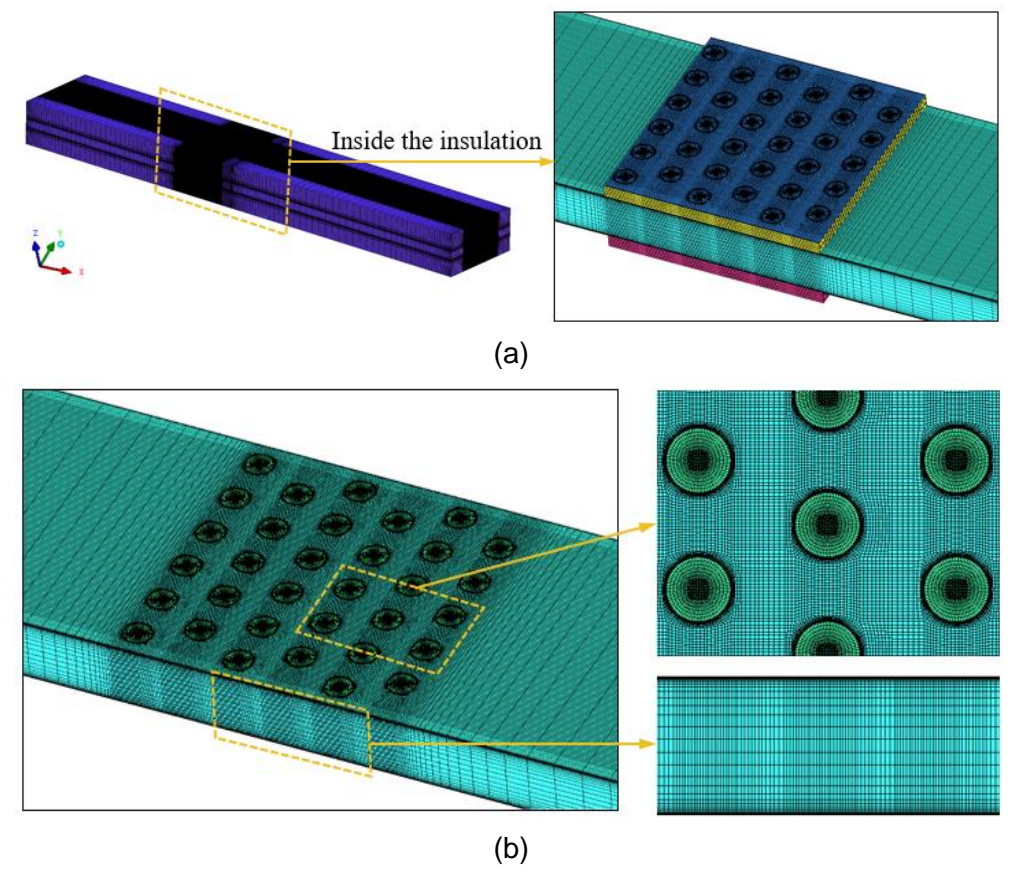


Figure 4 – Mesh of the computational domain.

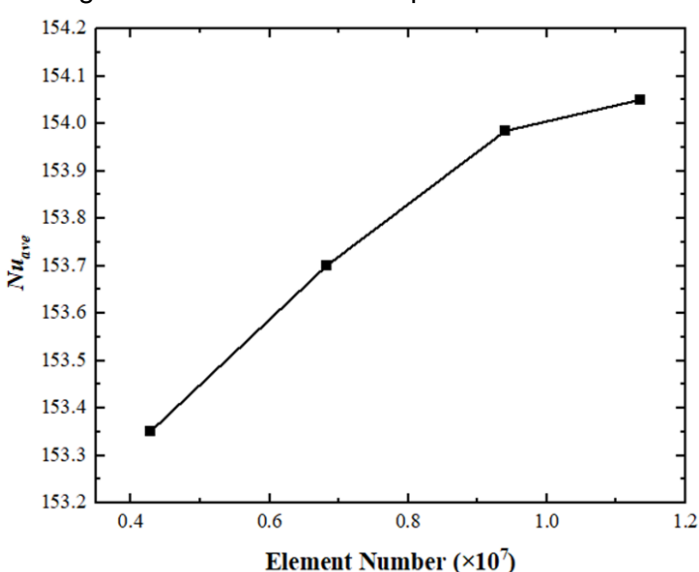


Figure 5 – Averaged Nusselt number of the channel under four grid systems.

4.3 Turbulence Model Verification

Choosing an appropriate turbulence model is of great importance to obtain accurate numerical results. Owing to the particularity of the experimental model, there is no published literature for comparative verification. Therefore, we designed a numerical model consistent with that of Wright et al. [20], and the corresponding data were calculated to select the turbulence model.

After the grid independence verification, five turbulence models (Standard κ - ϵ (Enhanced wall treatment), RNG κ - ϵ (Enhanced wall treatment), Realizable κ - ϵ (Enhanced wall treatment), Standard κ - ω and SST κ - ω) were selected to simulate the flow and heat transfer characteristics of the channel with the same geometries and boundary conditions as Wright's experiment as stated in section 2.1. The numerical results were then compared with Wright's experiment, as shown in Figure 7. It is found that the error between numerical results by using SST κ - ω turbulence model is within 7%. Therefore,

SST κ-ω is chosen as the suitable turbulence model for the present simulation work.

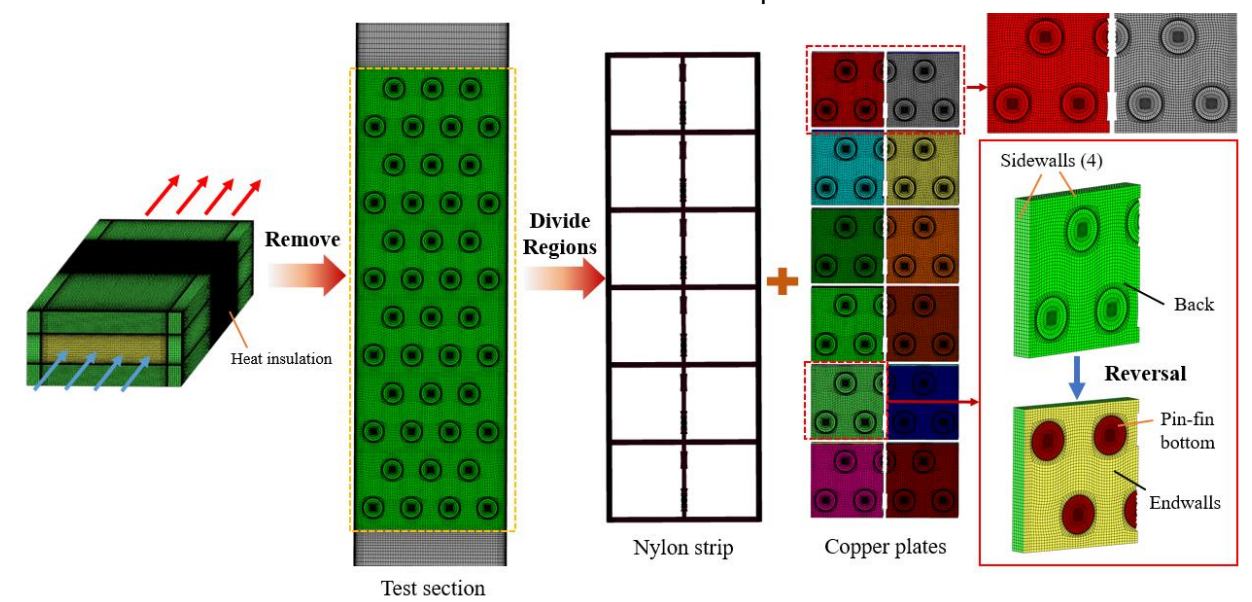


Figure 6 – Mesh of the computational domain of the model consistent with Wright's research [20].

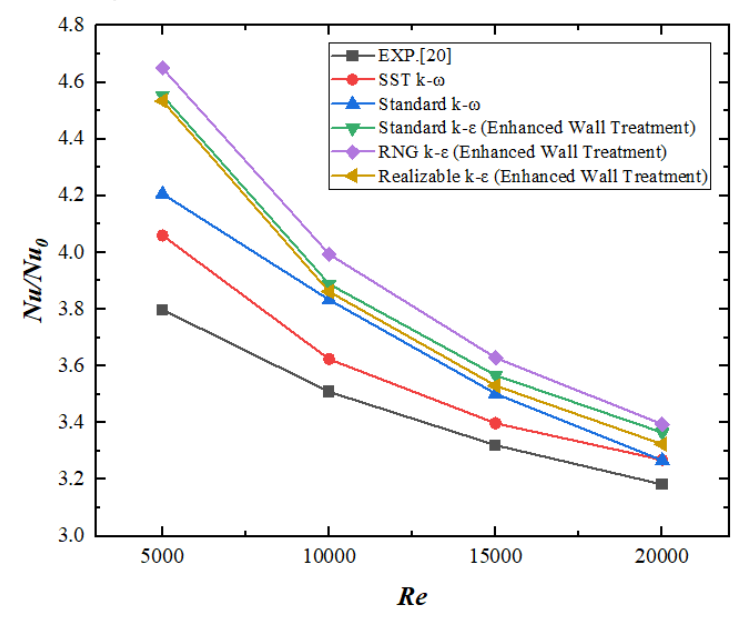


Figure 7 – Averaged Nusselt number ratio on the heated plates with different turbulence models.

5. Result and Discussion

5.1 Effect of pin-fin shape

5.1.1 Flow and temperature fields characteristics

Velocity distribution

As is stated before, the pin-fins in the channel perform as flow turbulators. At the leading edge of every pin-fin, a stagnation point is formed due to viscosity of fluid. Consequently, the flow breaks down into two distinct streams to flow around the pin-fin. And boundary layer develops on the wall of the pin-fin. The thickness of boundary layer is zero at the stagnation point, and then gradually increases along the pin-fins profile. The boundary layer separation occurs due to the contraction profile of the pin-fin near the trailing edge, and wake vortices are produced as a result. Figure 8(a) shows the velocity distribution on the central cross section in the height direction of z = 7.5 mm from row 1 to 3 of pin-fins near the axis of x. Figure 8(b) shows the enlarged view of wake vortices behind every kind of pin-fin. It can be seen that the separation phenomenon of circular pin-fin is the most serious. Less formation of wake region is observed in elliptic pin-fins followed by teardrop and circular pin-fins, which usually causes poor heat transfer performance.

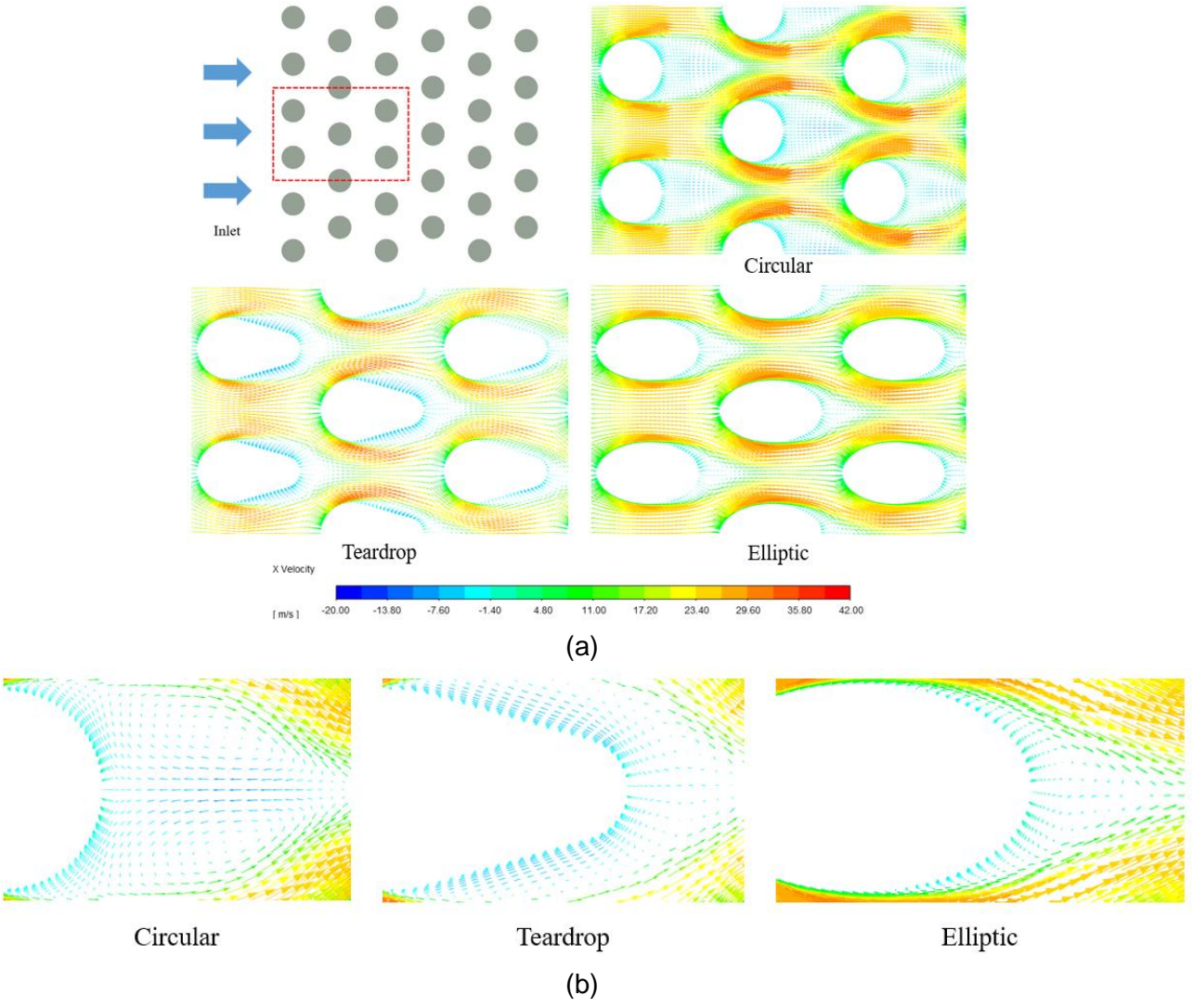


Figure 8 – Velocity distribution (unit: $m \cdot s^{-1}$) on the cross-section of z = 7.5 mm at Re = 20,000. Pressure distribution

Figure 9 shows pressure distribution at the cross-section of $z=7.5~\mathrm{mm}$ in the heated section on the condition of $Re=20{,}000$. The static pressure at the leading edge of pin-fins is very high due to the velocity stagnation. The flow rate is increased when air flows through the constructed cross-sectional area, and the pressure becomes lower. The pressure gradually decreases along the flow direction due to the frictional effects exerted by the channel wall and the pin-fins. The case with circular pin-fins has the highest overall pressure drop because of the same pressure outlet boundary condition across all cases.

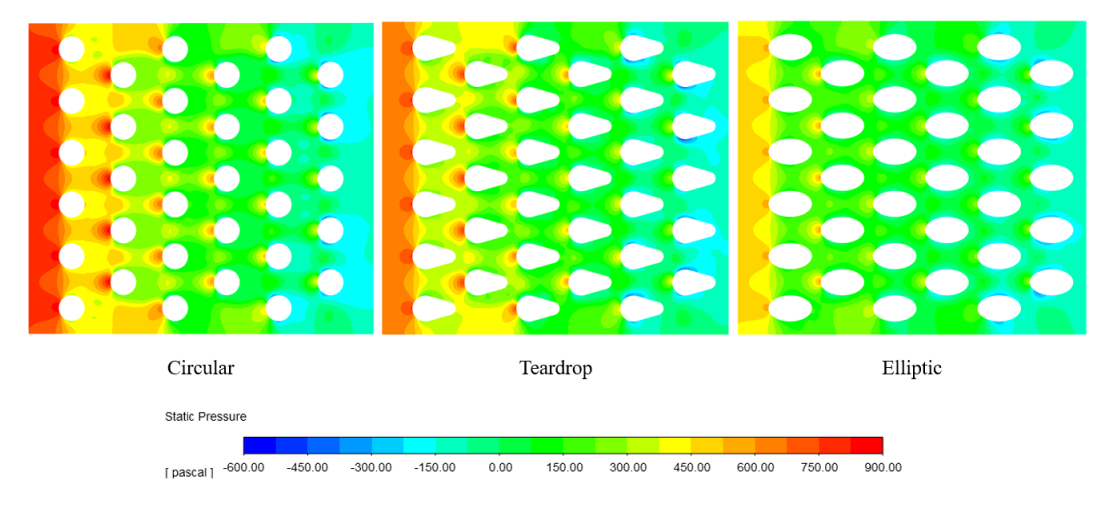


Figure 9 – Pressure distribution (unit: Pa) on the cross section of z = 7.5 mm at Re = 20,000.

5.1.2 Heat transfer characteristics and resistance characteristics

To study the variation of Nusselt number with rows of pin-fins, the heated wall and the pin-fin installed are divided into six parts along flow direction as shown in Figure 10(a), the averaged Nusselt numbers on every row part (Nu_{avr}) are compared. Figure 10(b) presents the change of Nusselt number with rows of pin-fins when Re = 5,000, 20,000 and 50,000. In general, Nusselt number increases as Reynolds number increases. The Nusselt number increases continuously in the region of the first three rows, then experiences a periodic fluctuation with row number. The phenomenon could be attributed to the fact that the odd number rows have 6 pin-fins, while the even number rows have 5 pin-fins. After the air flows through the first row of the pin-fins, the fluid turbulence intensity is enhanced continuously, which increases the rate of heat transfer. Following the first three rows downstream, the boundary layer on the heated wall is developed and interrupted periodically by the pin-fins, and the disturbance generated by 5 pin-fins is less strong than by 6 pin-fins. When Re is high, the influence of the pin-fin shape on the heat transfer becomes more obvious, the order of heat transfer enhancement by pin-fins is as teardrop, elliptic and circular.

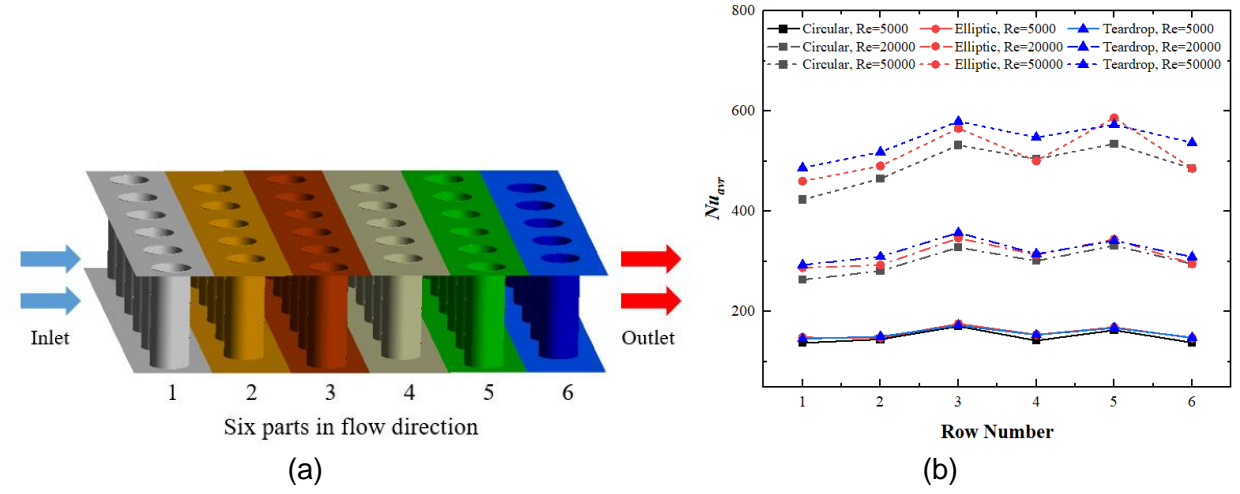


Figure 10 – Distribution of local Nusselt numbers along the flow direction (Nu_{avr}).

Figure 11(a) presents the averaged Nusselt number of the heated channel (Nu_{av}) with pin-fins designed in different shapes at various Reynolds numbers. The figure indicates that the averaged Nusselt number increases with Reynolds number increases. The effect of pin-fin shape becomes more significant on the heat transfer of the channel at high Reynolds numbers. Among them, the heat transfer effect of teardrop pin-fin is relatively high, while that of circular pin-fin is relatively low. To further understand the effect of pin-fin shape on the heat transfer characteristics of the channel, the paper calculates the ratios of the averaged Nusselt number of the channel (Nu_{av}) with pin-fins to the channel with smooth walls (Nu_0) as shown in Figure 11(b). It is notable that, as the flow velocity increases, the decrease of the heat transfer enhancement is shape at relatively low Reynolds numbers.

Figure 12 shows the ratios of the friction factor on the test channel (f) with different kinds of pin-fins to the friction factor (f_0) in the smooth channel. It is observed that pin-fins increases the friction factors greatly. In addition, f/f_0 is more sensitive to Re variations in case of circular pin-fin arrays, and the pressure loss they generate are 1.4 to 1.7 times that of elliptic pin-fins.

The thermal performance factor(Nu_{ave} / Nu_0 / (f / f_0) $^{1/3}$, TPF), as suggested by Gee and Webb [23], are presented in Figure 13, which provides a convenient way to evaluate the overall performances of pin-fin arrays with different shapes. For each shape, the TPF decreases with the increase of Re. The result indicates that, the values of TPF are round 1. Although the heat transfer enhances less by elliptic pin-fins when compared with teardrop pin-fins, elliptic pin-fins still shows slightly higher thermal performance values.

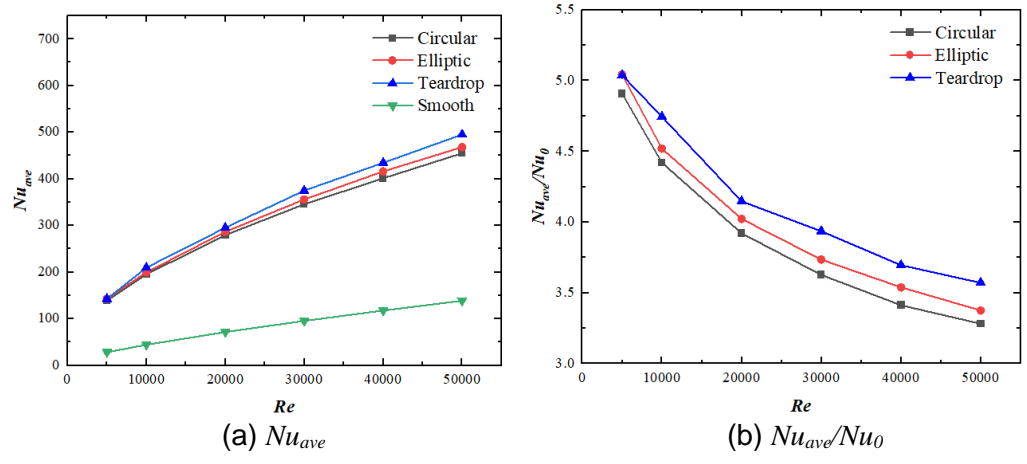


Figure 11 – Comparison of Nu_{ave} and Nu_{ave}/Nu_0 under different Reynolds numbers.

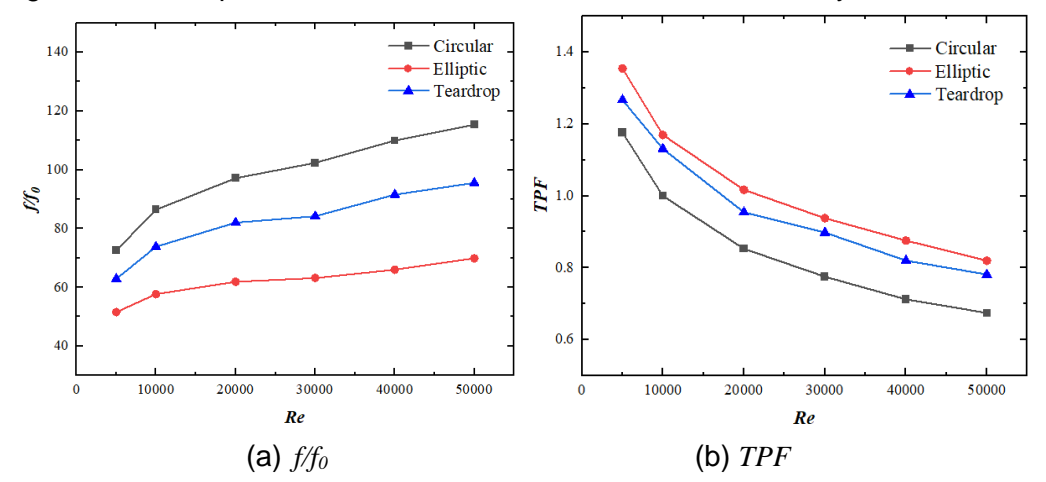


Figure 12– The f/f_0 and the *TPF* comparison of the test channel with different pin-fins.

5.2 Effect of streamwise spacing

Although circular pin-fins are widely used in the current actual turbine blade trailing edge cooling channel, the research above shows that the elliptic and teardrop pin-fin could bring about better overall thermal performance, which is close to each other. Due to the fact that the elliptical pin-fins are relatively convenient to design and process, further study should be conducted for channels with elliptic pin-fins. The research below presents the effect of streamwise spacing of elliptic pin-fins on the flow and heat transfer characteristics. The streamwise spacings in this section are 2, 2.5 and 3,

5.2.1 Flow characteristics

Figure 13 compares the streamwise velocity and streamline distributions in the cross-section of the channel utilizing the elliptical-shaped pins with various X/d at Re=20000. The cross-section is illustrated in Figure 14(a), which is located at the leading edge of the fourth row. When the X/d becomes larger, the streamwise velocity gradually decreases. In addition, with the increase of the streamwise spacing, the strength of vortices structures between adjacent two rows of pin-fins becomes weaker, which leads to the decrease of the interaction between the upstream and downstream rows.

5.2.2 Individual endwall and pin-fin heat transfer analysis

Endwall heat transfer

The endwall surface occupies nearly half of the heat transfer area in rectangular channels in the present study, as is shown in Table 5. So the endwall Nusselt number is critical to the heat transfer of the entire channel. Figure 14 presents the distributions that illustrates the Nu_e of the elliptical-shaped pin with different X/d, respectively. A great augmentation of heat transfer is observed in the U-shaped region at the leading edge of the pin-fin, which is attributed to the destruction of the boundary layer by the pin-fin. After passing through the pin-fin array, more turbulence is created, flow separation occurs along the pin-fins, horseshoe vortices associated with the pin-fin and endwall

further turbulate the flow-field and high heat transfer reattachment zones are created, which significantly increases the turbulence and results in an increase in heat transfer. As the spacing directly influences the effect of the pin-fin on the mainstream boundary layer, the endwall of small spacing channels has better heat transfer.

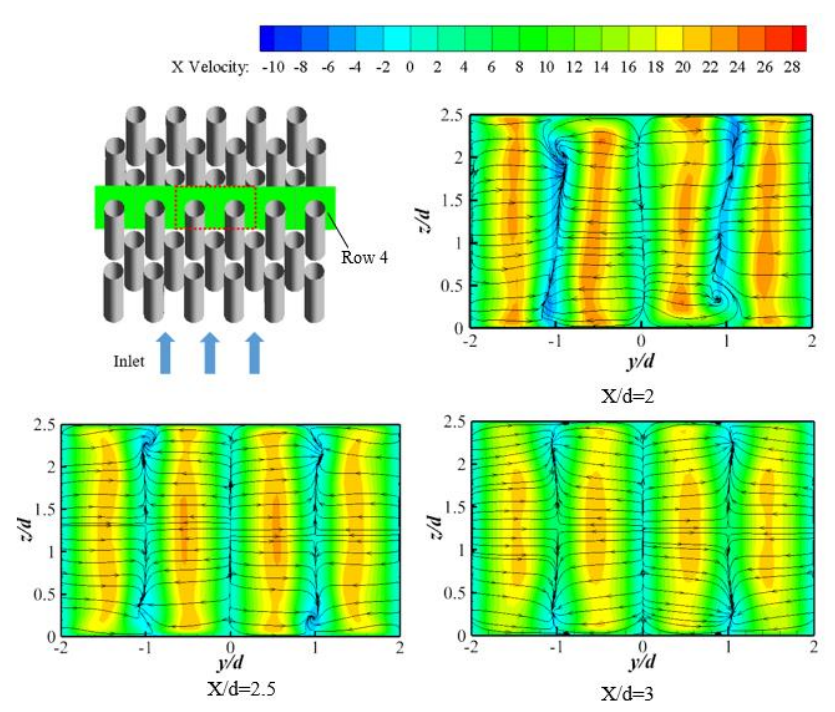


Figure 13 – Streamwise velocity and streamline at the leading edge of row 4 with various X/d. Table 5 –The heat transfer area percentage of the pin-fin and the endwall.

Table 6 The fleat traffeler	area percentage of the pil	Tim and the enawan.
X/d	Pin-fin	Endwall
2	49.15%	50.85%
2.5	44.13%	55.87%
3	40.04%	59.96%
		Nue 320 300 280 260 240 220 200
$Re_d = 9665$	Red = 9665	180 160
		140 120 100 80 60 40 20 0
$Re_d = 24164$	$Re_d = 24164$	
(a) $X/d = 2$	(b) $X/d = 3$	
- '		

Figure 14 – Contour of Nu_e on endwall.

Figure 15 illustrates the spanwise-averaged endwall Nusselt number of the elliptical-shaped pin with X/d = 2 and 3, respectively. The gray blocks in the figure represent the locations of the pin-fin rows. The increasing trend of Nu_e with the increasing Re_d can also be seen. Due to the accumulation of the disturbance on the main flow, the heat transfer performance of the endwall along the flow direction

first increases and then reaches nearly constant. It is noted that, for almost all the cases presented, the global peak occurs at the second or third flow. For the two configurations, the peak locations represent the leading edge of the pin-fin, since heat transfer is the strongest at the leading edge of pin-fins in the presence of horseshoe vortex and stagnation. It is observed that the trailing edge of pin-fins is quite different from the leading edge, which represents the wake region with low speed. By comparing the two configurations, it is found that the area influenced by the disturbance is larger when the streamwise spacing is small, so the heat transfer performance of the corresponding endwall is better on the whole, which is also shown in Figure 16.

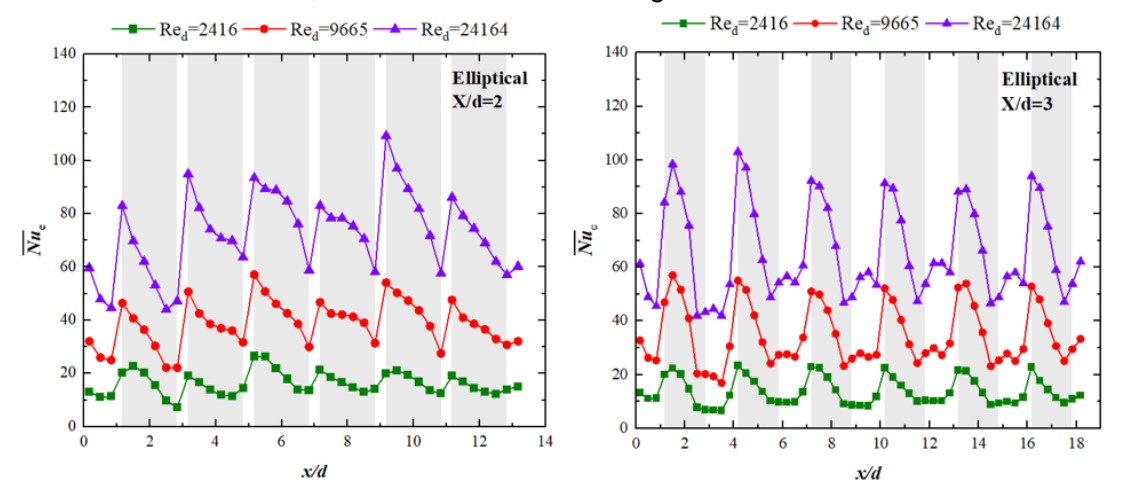


Figure 15 – Spanwise-averaged Nu_e of the elliptical-shaped pins with different X/d.

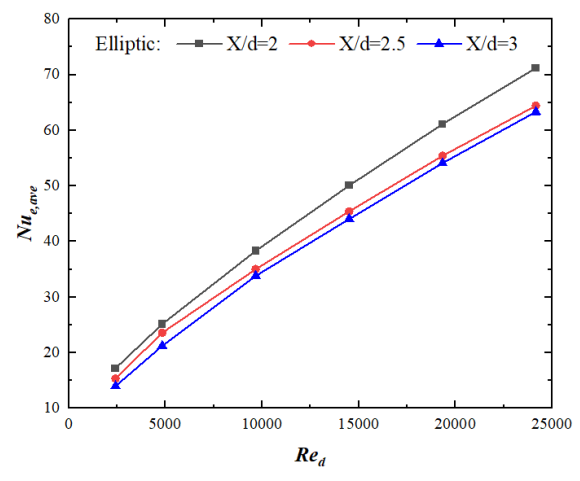


Figure 16 – Area-averaged endwall Nusselt number of the elliptical-shaped pins with different X/d. Pin-fin heat transfer

The pin surface also makes an essential contribution to the channel heat transfer. This section concentrates on the distribution and variation of the Nu_p of the elliptical-shaped pins with various X/d. A contour of Nu_p is shown in Figure 17(a). At the leading edge of the pin, the region near the stagnation point has the highest heat transfer due to the flow impact. At the trailing edge of the pinfin, the disturbance of the secondary flow in the wake region enhances the heat transfer in this region. At the same time, flow separation leads to lower heat transfer performance at the top of the pin, and the area near the minimum flow cross-section of the channel also has poor thermal performance. Figure 17(b) displays the pin Nusselt number (Nu_p) variation with the row number. In the flow direction, the continuous heating of the gas causes a descending trend in the heat transfer performance of the pin surface. Due to the impact of the mainstream, which is the main factor affecting the heat transfer of the pin-fin, the heat transfer enhances with the increase of Reynolds number, and the difference in heat transfer performance among the three channels is relatively small compared to the endwall. It is suggested that the heat transfer performance of the pin-fin is less affected by the streamwise spacing than the endwall.

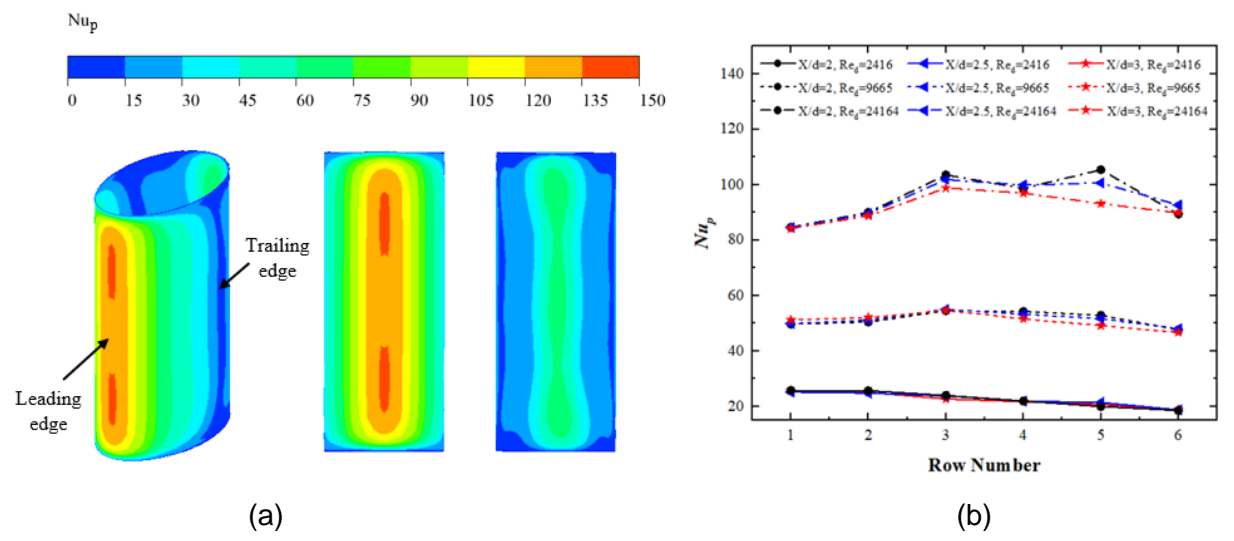


Figure 17 – Contour of Nu_p of the elliptical-shaped pins (X/d = 2.5, $Re_d = 9,665$) and Nu_p distribution along the flow direction.

The heat transfer of pin surface is hardly affected by the streamwise spacing, as is presented in Figure 18(a). Figure 18(b) displays the pin to endwall area-averaged Nusselt number ratio at different Reynolds numbers and X/d. When X/d=3, the ratio generally reduces with the increasing Re_d , which is mainly attributed to the slower growth of the Nu_p at higher Re_d . The highest ratio is found at the lowest Re_d and the largest X/d. However, this ratio keeps almost constant for the elliptical pin-fins with smaller X/d of 2 and 2.5. The ratio calculated in this study are ranged between 1.30 to 1.65, which is 10%-50% larger than that concluded in Chyu's study [17]. The difference can be attributed to the pin-fin shape used in the research.

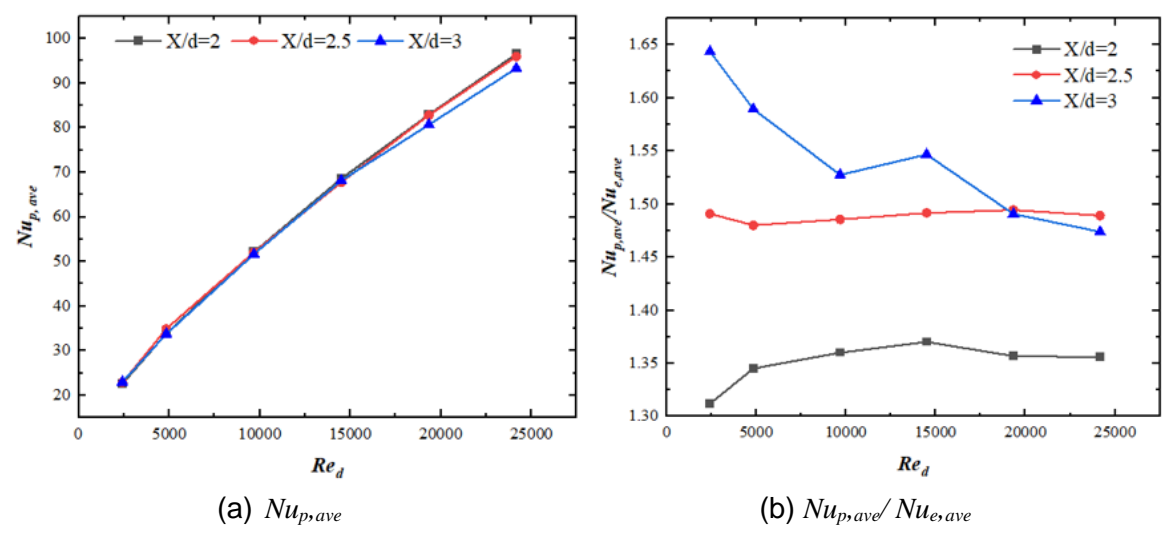


Figure 18– Comparison of $Nu_{p,ave}$ and the $Nu_{p,ave}/Nu_{e,ave}$ of elliptical-shaped pin-fins.

5.2.3. Overall heat transfer characteristics and resistance characteristics of the channel

Figure 19(a) depicts that with the increase of the streamwise spacing, the average Nusselt number of the channel decreases. Because when streamwise spacing increases, the influence of vortex structures caused by the front row of pin-fins on the leading edge areas of the rear row of pin-fins are weakened, making the secondary flow velocity between the two neighboring rows of pin-fins decrease, and the strength of vortex structure becomes weaker, the enhancement of the overall heat transfer also decreases, as shown in Figure 19(b). Figure 20 depicts the comparison of f/f_0 against Re for the elliptical pin-fins with different X/d. As shown in Figure 14, when the increase of the streamwise spacing, the strength of vortex structure between adjacent two rows pin-fins becomes weaker, and the interaction between the pin-fins decreases. Thus, a considerable decrease in pressure loss is caused. Figure 20 demonstrates the variations of TPF against Re. For elliptical shape of pin-fin, it is strongly suggested that elliptical pin-fins combined with the arrangement of X/d = 2 has the highest efficiency among the various X/d studied in this paper.

X/d=2

-X/d=2.5

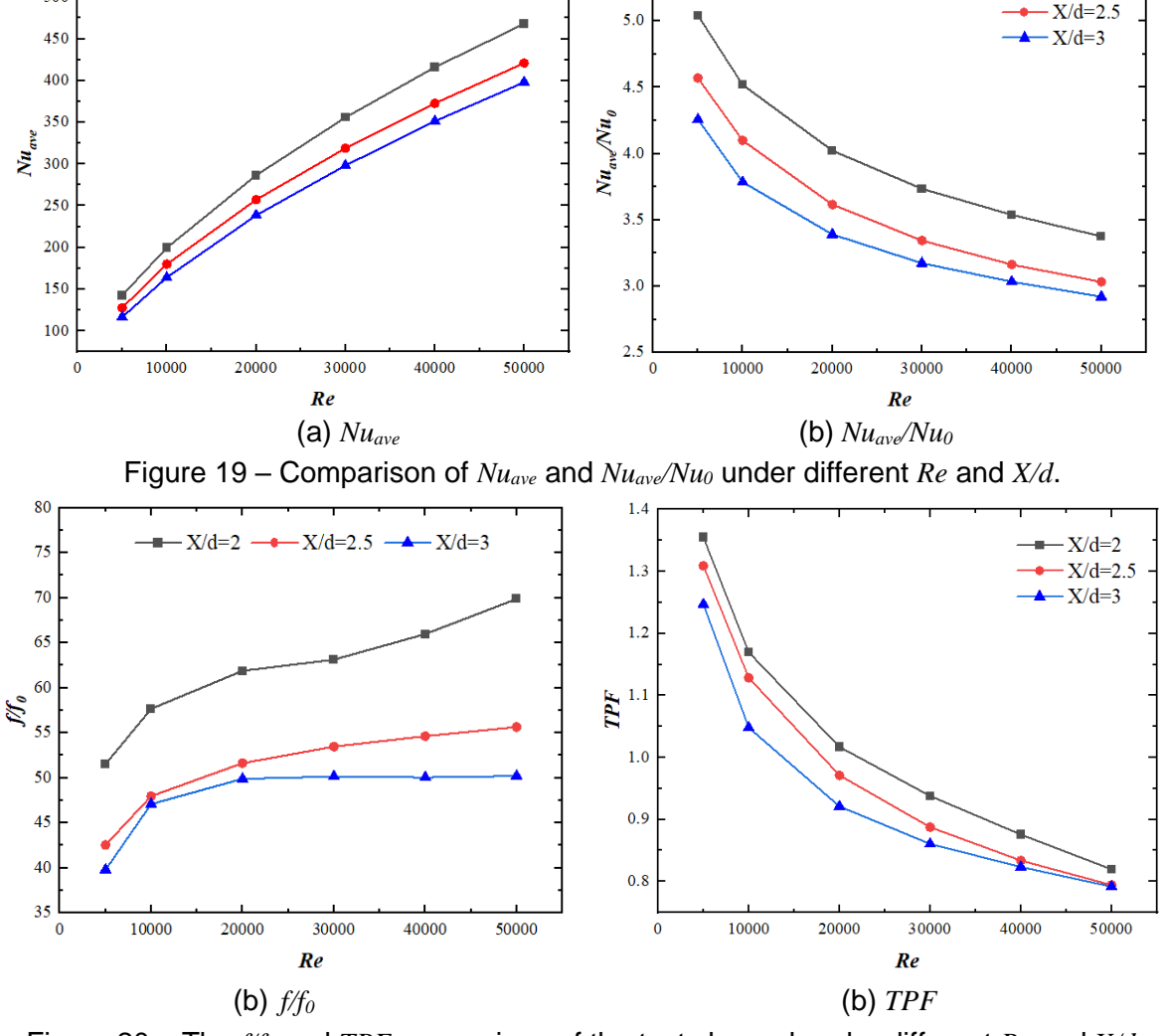


Figure 20 – The f/f_0 and TPF comparison of the test channel under different Re and X/d.

6. Conclusions

500

The effects of shape and streamwise spacing of pin-fins on the flow and heat transfer characteristics in the rectangular channel are numerically investigated. The conclusions are as follows:

- (1) SST κ-ω turbulence model is suitable to be used in simulating the heat transfer problem combined with cylinder heat transfer and endwall heat transfer in the channel with pin-fins.
- (2) In the same flow and geometrical conditions, elliptic pin-fin will bring about better overall thermal performance of the channel than teardrop and circular pin-fins.
- (3) The channel with elliptic pin-fins at X/d = 2 has the best overall thermal performance than other arrangements of elliptic pin-fins in this study (X/d = 2.5, X/d = 3).
- (4) For the elliptical pin-fins with H/d = 2.5, Nu_p is less affected by streamwise spacing than Nu_e , and the ratio of $Nu_{p,ave}/Nu_{e,ave}$ ranges from 1.30 to 1.65 for the elliptic pin-fins studied in this article.

Funding

The work presented in this paper is supported by the National Science and Technology Major Project (J2019-III-0007-0050).

Contact Author Email Address

mailto: charlotte384@stu.xitu.edu.cn

Copyright Statement

The authors confirm that they, and/or their company or organization, hold copyright on all of the original material included in this paper. The authors also confirm that they have obtained permission, from the copyright holder of any third party material included in this paper, to publish it as part of their paper. The authors confirm that

they give permission, or have obtained permission from the copyright holder of this paper, for the publication and distribution of this paper as part of the ICAS proceedings or as individual off-prints from the proceedings.

References

- [1] Du W, Luo L, Jiao Y, et al. Heat transfer in the trailing region of gas turbines—A state-of-the-art review. *Applied Thermal Engineering*, 199: 117614, 2021.
- [2] Chyu M K, Goldstein R J. Influence of an array of wall-mounted cylinders on the mass transfer from a flat surface. *International journal of heat and mass transfer*, 34(9): 2175-2186, 1991.
- [3] S.A. Lawson, A.A. Thrift, K.A. Thole, A. Kohli, *Heat transfer from multiple row arrays of low aspect ratio pin fins. Int. J. Heat Mass Tran*, 54 (17–18) 4009–4109, 2011.
- [4] Ostanek J K, Thole K A. Effects of varying streamwise and spanwise spacing in pin-fin arrays. *Turbo Expo: Power for Land, Sea, and Air*, 44700: 45-57, 2012.
- [5] Z. Chen, Q. Li, D. Meier, H.J. Warnecke, Convective heat transfer and pressure loss in rectangular ducts with drop-shaped pin fins. *Heat Mass Transf*, 33 (3) 219–224, 1997.
- [6] Sahiti N, Lemouedda A, Stojkovic D, et al. Performance comparison of pin fin in-duct flow arrays with various pin cross-sections. *Applied thermal engineering*, 26(11-12): 1176-1192, 2006.
- [7] O. Uzol, C. Camci, Heat transfer, pressure loss and flow field measurements downstream of staggered two-row circular and elliptical pin fin arrays, *ASME J. Heat Transfer*, 127 (5) 458–471, 2005.
- [8] Xu J, Zhang K, Duan J, et al. Systematic comparison on convective heat transfer characteristics of several pin fins for turbine cooling. *Crystals*, 11(8): 977, 2021.
- [9] Corbett, T. M., Thole, K. A., and Bollapragada, S. Impacts of Pin Fin Shape and Spacing on Heat Transfer and Pressure Losses. *ASME. J. Turbomach*, 145(5): 051014, 2023.
- [10]G. J. VanFossen, Heat-transfer coefficients for staggered arrays of short pin fins. *J. Eng. Gas Turbines Power*, vol. 104, no. 2, pp. 268–274, 1982.
- [11] Chyu M K, Siw S C, Moon H K. Effects of height-to-diameter ratio of pin element on heat transfer from staggered pin-fin arrays. *Turbo Expo: Power for Land, Sea, and Air.* 48845: 705-713, 2009.
- [12] Weigand B, Semmler K, von Wolfersdorf J. Heat Transfer Technology for Internal Passages of Air-Cooled Blades for Heavy–Duty Gas Turbines. *Annals of the New York Academy of Sciences*, 934(1): 179-193, 2001.
- [13] Metzger D E, Berry R A, Bronson J P. Developing heat transfer in rectangular ducts with staggered arrays of short pin fins. 1982.
- [14] Jin, W., Wu, J., Jia, N., Lei, J., Ji, W., & Xie, G. Effect of shape and distribution of pin-fins on the flow and heat transfer characteristics in the rectangular cooling channel. *International Journal of Thermal Sciences*, *161*, 106758, 2021.
- [15] Lee, Chien-Shing, et al. Effects of High Heating Loads on Unsteady Flow and Heat Transfer in a Cooling Passage with a Staggered Array of Pin Fins. *Turbo Expo: Power for Land, Sea, and Air.* Vol. 58646, 2019.
- [16]D. E. Metzger, C. S. Fan and S. W. Haley, Effects of pin shape and array orientation on heat transfer and pressure loss in pin fin arrays. *J. Eng. Gas Turbines Power*, vol. 106, no. 1, pp. 252–257, 1984.
- [17]M. K. Chyu, Y. C. Hsing, T. I.-P. Shih and V. Natarajan, Heat transfer contributions of pins and endwall in pin-fin arrays: effects of thermal boundary condition modeling. *J. Turbomach.*, vol. 121, no. 2, pp. 257–263, 1999.
- [18]M. E. Lyall, A. A. Thrift, K. A. Thole and A. Kohli, Heat transfer from low aspect ratio pin fins, *J. Turbomach.*, vol. 133, no. 1, p. 011001, 2011.
- [19] Deng H W, Wang Y B, Deng W, et al. Effect of pin-fin material on heat transfer and flow resistance characteristic of rectangular channel. *Advanced materials research*, 663: 490-496, 2013.
- [20] Wright L M, Lee E, Han J C. Effect of rotation on heat transfer in rectangular channels with pin-fins. *Journal of thermophysics and heat transfer*, 18(2): 263-272, 2004.
- [21]Li W, Yang L, Ren J, et al. Effect of thermal boundary conditions and thermal conductivity on conjugate heat transfer performance in pin fin arrays. *International Journal of Heat and Mass Transfer*, 95: 579-592, 2016.
- [22]Zhang X, You R, Li H, et al. Enhancing heat transfer in a rotating droplet-shaped pin-fins channel: Investigating the influence of rotational radius ratio and temperature ratio. *Applied Thermal Engineering*, 2024.
- [23] Gee D L, Webb R L. Forced Convection Heat Transfer in Helically Rib-Roughened Tubes. *International Journal of Heat & Mass Transfer*, 23(8):1127-1136, 1980.